

# CROSS SECTIONS FOR PRINCIPAL CHANNELS WITH ONE NEUTRAL PARTICLE IN 32 GeV/c $K^-p$ INTERACTIONS (CERN-Soviet Union Collaboration)

BY M. S. LEVITSKY, A. M. MOISEEV, S. G. SILINSKAIA, E. A. STARCHENKO,  
D. I. PATALAKHA, S. V. CHEKULAEV

Institute for High Energy Physics, Serpukhov, USSR

U. GENSCH, M. WALTER

Institut für Hochenergiephysik der Akademie der Wissenschaften der DDR, Berlin-Zeuthen, GDR

J. MACNAUGHTON AND M. MARKYTAN

Institut für Hochenergiephysik der Österreichischen Akademie der Wissenschaften\*, Vienna, Austria

(Received November 12, 1982; final version received March 21, 1983)

In this paper a procedure for separating channels with one neutral particle produced in 32 GeV/c  $K^-p$  interactions is described. Cross section values for the reactions with one  $\pi^0$ ,  $\bar{K}^0$  unseen or neutron are presented, and their energy dependence is shown.

PACS numbers: 13.85.-t

## 1. Introduction

A number of current problems in high energy physics are related to the investigation of channels with one neutral particle [1, 2]. The possibility of separating such channels using conservation of energy and momentum has always been extensively utilized in analysis of bubble chamber data at low and intermediate energies. However in contrast to exclusive reactions having only charged particles in the final states, which can be separated on the basis of four constraint kinematic fits (4c fits), reactions with one undetected neutral particle can be separated only on the basis of one constraint kinematic fits (1c fits).

With increasing energy the separation of channels with one neutral particle becomes less reliable, because the errors in the reconstruction of the trajectories of the charged

---

\* Supported in part by Österreichischer Forschungsrat.

particles become larger. In  $K^-p$  interactions such final states have previously been separated at energies up to 16 GeV [2].

In experiments with the Mirabelle bubble chamber the separation of 1c fit channels (i.e. channels with one unseen neutral particle) is more difficult because of the large momentum of the incident particles and the reduced accuracy of reconstruction of events in the fiducial volume of the chamber due to its design characteristics. A study of the inherent possibilities of this chamber, undertaken for the pp experiment at 69 GeV/c [3], demonstrated that at this energy it was possible to separate 4c fit channels, but the separation of 1c fit channels was almost impossible.

In this paper results of a detailed investigation of the possibilities of separating 1c fit channels in the 32 GeV/c  $K^-p$  experiment are presented. During the analysis of this experiment at IHEP both 4c fit and 1c fit hypotheses were included in the "GRIND" program for topologies of low multiplicity ( $n_{ch} \leq 6$ ).

In order to obtain undistorted parameters for reconstructed tracks, corrections for systematic distortions, calculated using the method described in Ref. [4], were applied to the results of the geometrical reconstruction program before calculation in program "GRIND". On the basis of the results of the "GRIND" calculations the following exclusive channels were separated:

$$K^-p \rightarrow K^-p + m(\pi^+\pi^-) + \pi^0 \quad (1)$$

$$K^-p \rightarrow \bar{K}_{seen}^0 p + m(\pi^+\pi^-) + \pi^0 \quad (2)$$

$$K^-p \rightarrow \pi^-p + m(\pi^+\pi^-) + K_{unseen}^0 \quad (3)$$

$$K^-p \rightarrow K^-\pi^+ + m(\pi^+\pi^-) + n, \quad (4)$$

where  $m = 0, 1, 2$ .

Several systematic problems related to the separation of these channels, the analysis of ambiguous events, the determination of the principal sources of contamination and the experimental data for the evaluation of the cross sections for these reactions will be discussed below. For simplicity reaction (1) will be treated as an example, which is the principal object of this investigation.

## 2. Experimental procedure

The input data for this investigation were the 1c fit events obtained at IHEP from about 50000 primary interactions (the complete statistics of the experiment is 123000 events) in the 32 GeV/c  $K^-p$  experiment. The events were measured on HPD machines or precision measuring projectors and were calculated with the standard programs "H-GEOM"- "GRIND"- "SLICE". Details of the data reduction can be found in a previous publication of the collaboration [5].

The best 1c fit hypotheses with  $\chi^2 < 10$  limited to a maximum of four and excluding those hypotheses whose probabilities were less than 1/3 that of the best hypothesis were written on DST in the order of decreasing probability  $P(\chi^2)$ . If a particular hypothesis

had a probability  $P(\chi^2)$  more than three times larger than the corresponding probabilities for all other hypotheses, it was considered unambiguous.

In Fig. 1 the distribution  $P(\chi^2)$  is shown for events for which the best hypothesis corresponds to reactions (1) with  $m = 0, 1, 2$ . As can be seen from this figure, this distribution is almost uniform in the region  $P(\chi^2) > 0.1$ , but has a maximum at small probabilities which could be caused by contamination from other channels. Therefore only events for which the best 1c fit hypothesis has  $P(\chi^2) > 0.07$  (the boundary for this cut is shown in Fig. 1 by the dashed line) are considered further.

In Fig. 2 (upper row) the distribution in  $M_{\text{mis}}^2$  is shown for events for which the best hypothesis corresponds to reaction (1) (the dashed histogram shows the corresponding

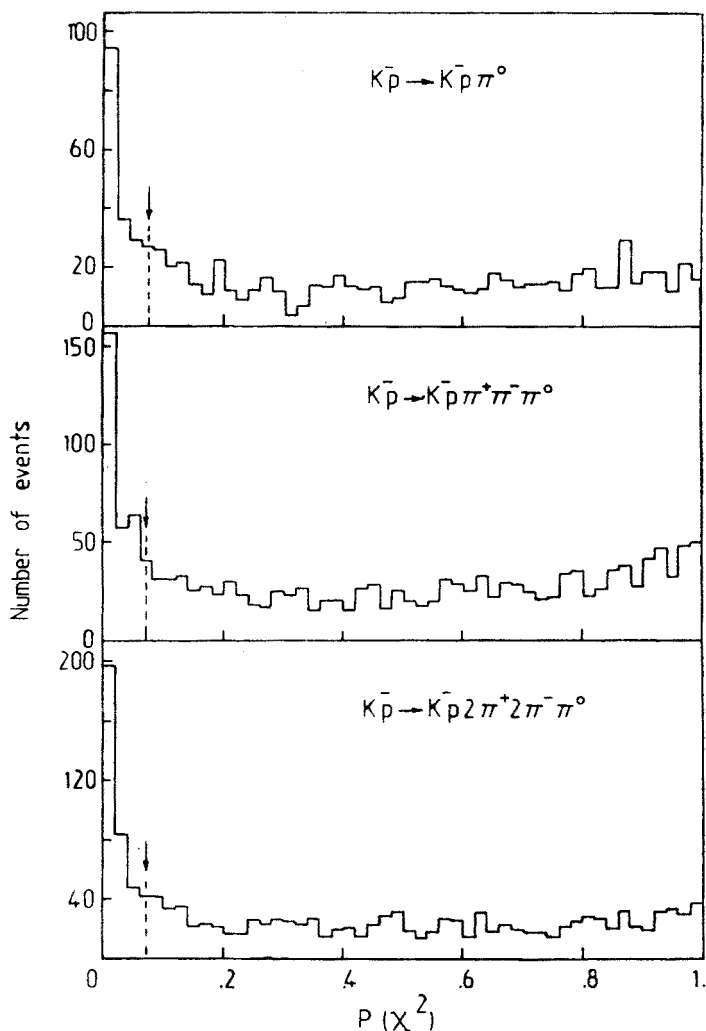


Fig. 1. Probability distributions for reactions (1) with  $m = 0, 1, 2$ . The dashed lines show the position of the cutoff chosen for the selection of 1c fit reactions

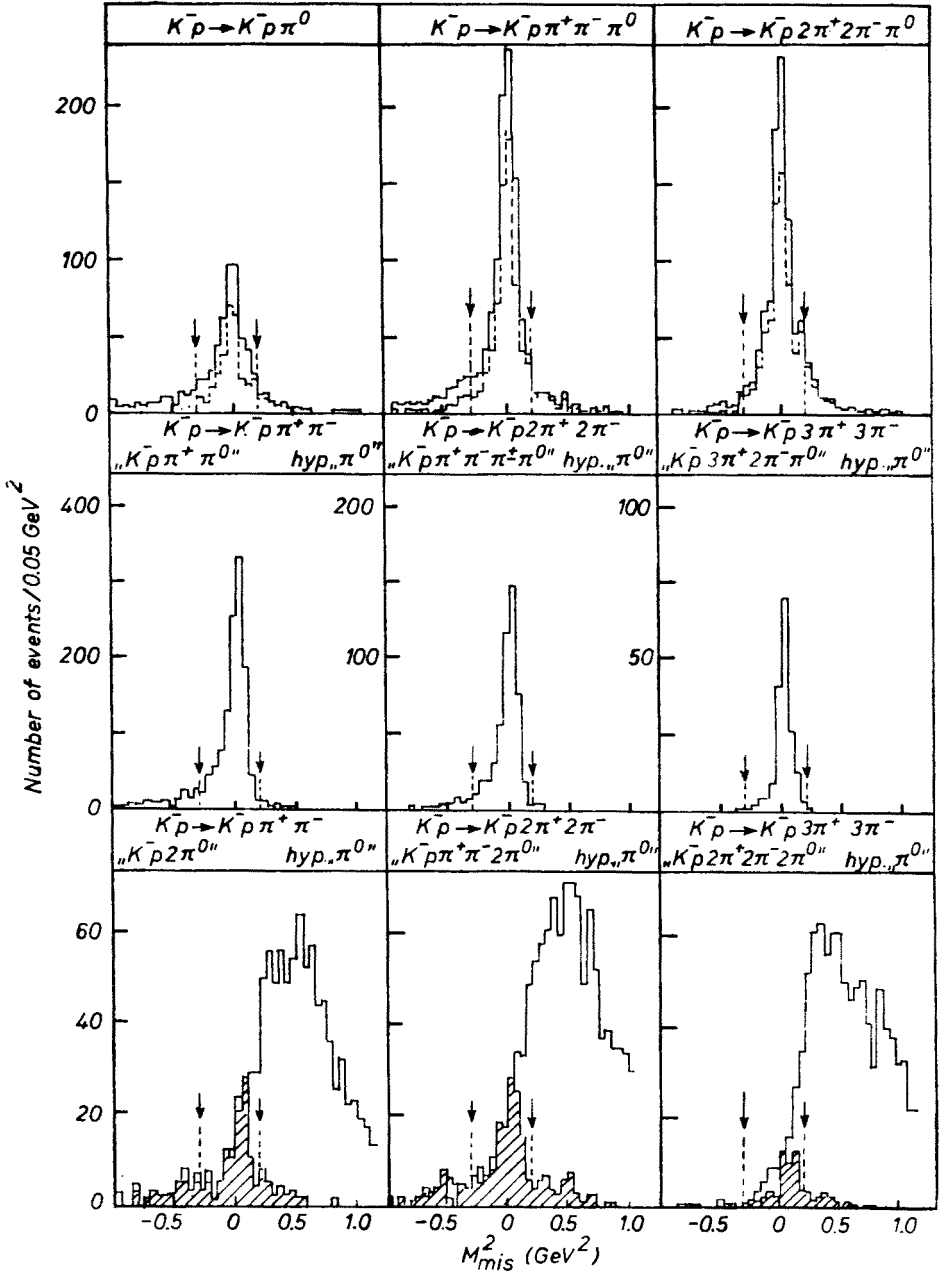


Fig. 2. Missing mass distributions for reactions (1) with  $m = 0, 1, 2$  obtained from real events (upper row) and from events, which satisfy four constraint fits, but have been suitably modified to simulate reactions with one  $\pi^0$  (middle row) and two  $\pi^0$ 's (bottom row). The dashed histograms in the upper row correspond to events fitting reaction (1) uniquely; the solid histograms in the upper and middle rows and the shaded histograms in the lower row correspond to real or simulated events where the best fit is the reaction (1) ( $P(\chi^2) > 0.07$ ). The solid histograms in the lower row have no selection on  $P(\chi^2)$ . The dashed lines and arrows show the position of the missing mass cutoff chosen for further selection

histogram for events fitting reaction (1) unambiguously). A clear  $\pi^0$  signal is seen for all topologies; the width of the  $\pi^0$  peak is smaller for topologies of larger multiplicity which is related to the greater measurement precision for slower tracks. On the whole the resolution in  $M_{\text{mis}}^2$  in this experiment does not differ significantly from the resolution obtained in the 14.3 GeV/c K<sup>-</sup>p experiment (the ratio of the width to the half height  $dN/d(M_{\text{mis}}^2)$  for both 32 and 14.3 GeV/c for two prong events from reaction (1) is equal to 1.3). But even for 6 prong events with a  $\pi^0$ , the width of the  $M_{\text{mis}}^2$  distribution is large enough to overlap with the missing mass of  $2\pi^0$ 's and a  $\bar{K}^0$  meson, so that some of the events assigned to reaction (1) may originate from the corresponding reaction with  $2\pi^0$ 's or from reaction (3). As is seen in Fig. 3 (upper row) where the number of unique events fitting reactions (1), (3), (4) respectively are plotted, and where also the numbers of events having various specific ambiguities are shown, there are a significant number of ambiguous events. There is an especially large number of events which have nearly the same probability for  $\pi^0$  and  $\bar{K}^0$  reactions. With increasing multiplicity the fraction of ambiguous events decreases.

As lower energy investigations have shown, the principal sources of ambiguities for 1c fit events are interchanges among the channels (1), (3), (4) and contamination from channels with more than one neutral particle [6] which can also contribute to 1c fit events classified as unambiguous according to the criteria described above. Therefore in order to evaluate the quality of 1c fit events the principal sources of contamination (separation error of the second type) and loss (separation error of the first type) were carefully investigated for events lying in kinematic regions close to those identified as 1c fit events.

For this reason we studied 4c fit events corresponding to the reactions

$$K^-p \rightarrow K^-p + m(\pi^+\pi^-), \quad (5)$$

where  $m = 1, 2, 3$ . Discarding in these events one or several charged particles of various types, we created samples of test simulated events with one ( $\pi^0$ ,  $\bar{K}^0$ ,  $n$ ) or several different missing neutral particles. Thus the multiplicity of charged particles in the test sample was one larger than the multiplicity of the corresponding simulated 1c fit channel. The distributions in  $M_{\text{mis}}^2$  are shown in Fig. 2 for test events with a single  $\pi^0$  (middle row) and  $2\pi^0$  (lower row). The solid histograms in the lower row in Fig. 2 have no selection on  $\chi^2$ ; all other histograms in Fig. 2 have  $P(\chi^2) > 0.07$  for reaction (1). The distributions in  $M_{\text{mis}}^2$  for events with one  $\pi^0$  give an impression of the real resolution in  $M_{\text{mis}}^2$  for the K<sup>-</sup>p experiment at 32 GeV/c. For each test event the quantity  $D^2$  was calculated for each 1c fit hypothesis according to the following formula

$$D^2 = (M_{\text{mis}}^2 - M_{\text{neutr}}^2)^2 / (\Delta M_{\text{mis}}^2)^2,$$

where  $M_{\text{mis}}^2$  — missing mass squared with respect to the remaining charged particles,  $M_{\text{neutr}}^2$  — mass squared of the simulated neutral particles,  $\Delta M_{\text{mis}}^2$  — error on missing mass squared.

For a 1c fit hypothesis the value of  $D^2$  is closely related to the  $\chi^2$ , since in this case only one constraint equation remains. Subsequently, as in the real experiment, the four best hypotheses were selected, the ratios of the probabilities of which were not permitted

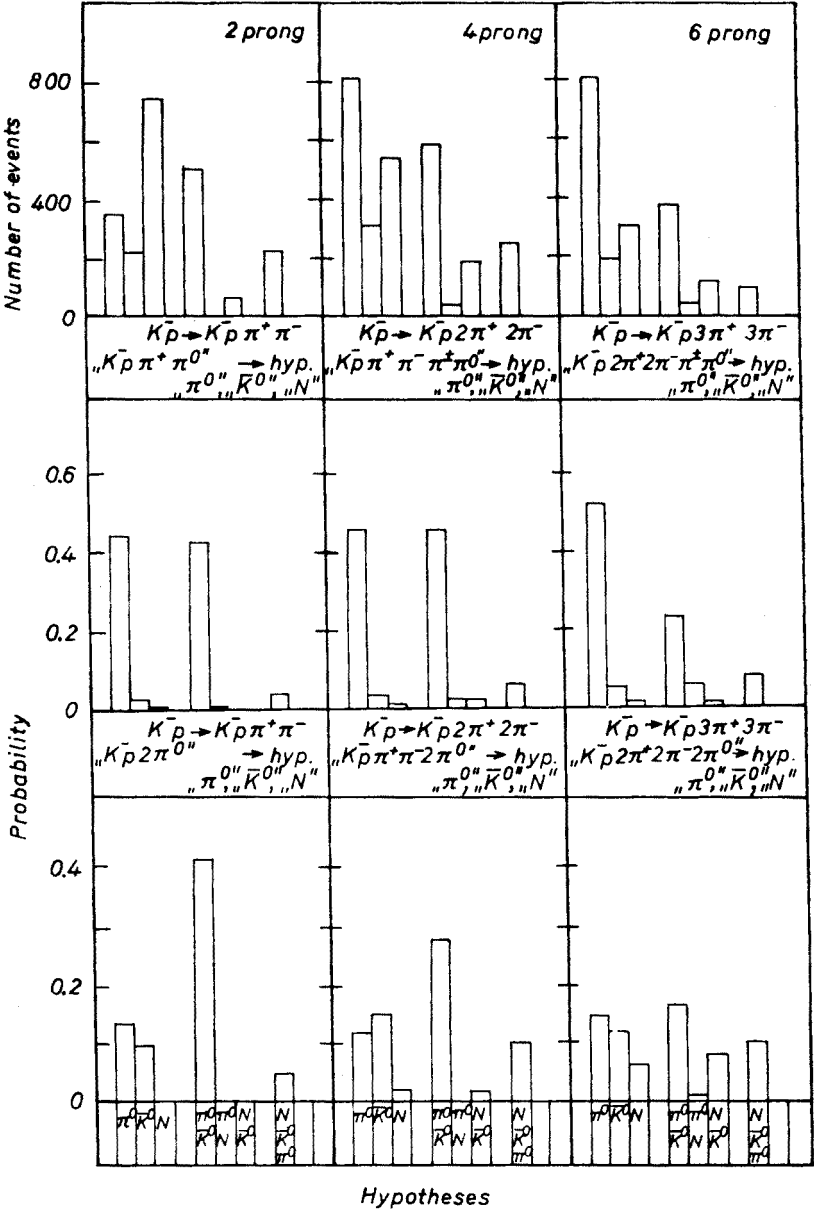


Fig. 3. Distributions showing how many events have a unique fit with  $P(\chi^2) > 0.07$  to channels with a  $\pi^0$ ,  $\bar{K}^0$ ,  $n$  and how many have the following ambiguities:  $\pi^0 - \bar{K}^0$ ,  $\pi^0 - n$ ,  $n - \bar{K}^0$  and  $\pi^0 - \bar{K}^0 - n$ . In the upper row where real events are shown, the number of events in each category is plotted. The middle and bottom rows correspond to events which satisfy four constraint fits, but have been suitably modified to simulate reactions with one  $\pi^0$  (middle row) and two  $\pi^0$ 's (bottom row). In the middle and bottom rows the ratios of the number of simulated events in each category to the total number of simulated events are plotted

to exceed three, and value of  $D^2$  itself was not allowed to exceed three (corresponding to  $P(D^2) > 0.07$ ).

In Fig. 3 the numbers of test events with one  $\pi^0$  (middle row) and two  $\pi^0$ 's (lower row), for which one or several 1c fit hypotheses were accepted, are shown as an example. From Fig. 3 it is seen that for test events with one  $\pi^0$  in a large number of cases (ranging from 50% for 2-prongs to 20% for 6-prongs) two 1c fit hypotheses (with  $\pi^0$  and  $\bar{K}^0$ ) were accepted.

Moreover, in the same figure it is seen that events with  $2\pi^0$ 's rather often satisfy a 1c fit hypothesis with one  $\pi^0$ , although usually they satisfy two hypotheses ( $\pi^0$  and  $\bar{K}^0$ ). For further analysis in order to reduce the contamination of  $2\pi^0$  events in the channels with one  $\pi^0$  an additional cut was made on  $M_{\text{mis}}^2$ : ( $-0.3 \text{ GeV}^2 < M_{\text{mis}}^2(\pi^0) < 0.2 \text{ GeV}^2$ ). As seen in Fig. 2 (the dashed lines show the boundaries of the cut) for test events with one  $\pi^0$  meson (middle row) and  $2\pi^0$  mesons (shaded region in the bottom row), for which the best hypothesis is reaction (1), this cut is the minimal one still permitting a detailed analysis of the contamination. Corresponding cuts were made for  $M_{\text{mis}}^2$  in reactions (3) and (4) ( $0.0 \text{ GeV}^2 < M_{\text{mis}}^2(\bar{K}^0) < 0.5 \text{ GeV}^2$ ,  $0.0 \text{ GeV}^2 < M_{\text{mis}}^2(n) < 2.0 \text{ GeV}^2$ ).

The probability (in %) is shown in Table I for test events simulating reactions (1), (3) and (4), after applying the cuts on  $D^2$  and  $M_{\text{mis}}^2$  described above, to be assigned to the 1c fit channels with  $\pi^0$ ,  $\bar{K}^0$ ,  $n$ . The upper number corresponds to selection according to the best hypothesis, the lower one to unambiguously separated hypotheses. It is seen that for events where the true hypothesis is uniquely selected, the contamination from competing channels is considerably reduced, however, such a selection leads to a significant (up to 50%) loss of statistics in the channel under investigation. The probabilities in various channels were calculated for determination of the contamination of the 1c fit channel under investigation using the corresponding channel with a  $K^+K^-$  pair.

In Table II the probabilities are shown for final states with several neutral particles being assigned to the final states (1), (3), (4) (upper and lower figures have the same meaning as in Table I).

### 3. Determination of cross sections

In order to obtain absolute values for the contamination it is necessary at least to estimate the cross sections for reactions with several neutral particles. We obtained such estimates for the channels with  $\bar{K}_{\text{sec}}^0\pi^0$  and  $\bar{K}^0, \pi^0, n$  from our experiment by successive approximation and for the channels with  $\bar{K}^0 + m\pi^0$  and  $m\pi^0$  with  $m > 1$ , we used the ratios of semiinclusive cross sections with various numbers of  $\pi^0$ 's from  $\pi^\pm p$  experiments at 10.1 and 15 GeV/c [7]. Cross sections for channels with  $n + m\pi^0, n + \bar{K}^0 + m\pi^0, m > 1$ , cannot be estimated in this way, because there is no experimental information for the case  $m = 1$ . Rough estimates for the channels with  $m = 1$  were made from general physical ideas. These values do not have a substantial effect on the results. For the case  $m > 1$  the assumption was made that the ratios of cross sections for formation of various numbers of  $\pi^0$ 's with fixed final state particles corresponding to channels (1)–(4) has approximately the same form as the semiinclusive cross sections. On the basis of experimental data for  $\pi^\pm p$  interactions at 15 GeV/c, the average value  $\langle n_{\pi^0} \rangle = 1.8$  which agrees well with the

TABLE I

1c fit hypotheses assigned according to selection criteria	$K^-p+\pi^0$ + charged $\pi$ mesons (%)	$\pi^-p+\bar{K}^0$ + charged $\pi$ mesons (%)	$K^-\pi^++n$ + charged $\pi$ mesons (%)
Channels simulated			
$K^-p\pi^\pm\pi^0$	$67\pm2$	$15\pm1$	$1\pm1$
	$48\pm2$	$6\pm1$	$1\pm1$
$\pi^-p\pi^+\bar{K}^0$	$6\pm1$	$65\pm3$	$1\pm1$
	$1\pm1$	$49\pm2$	$1\pm1$
$K^-\pi^+\pi^-n$	$7\pm1$	$6\pm1$	$49\pm2$
	$3\pm1$	—	$48\pm2$
$K^-p\pi^+\pi^-\pi^\pm\pi^0$	$67\pm3$	$15\pm1$	$4\pm1$
	$48\pm2$	$5\pm1$	$2\pm1$
$\pi^-p2\pi^+\pi^-\bar{K}^0$	$11\pm2$	$65\pm6$	$3\pm1$
	$3\pm1$	$44\pm4$	$2\pm1$
$K^-2\pi^+2\pi^-n$	$8\pm2$	$9\pm2$	$58\pm5$
	$2\pm1$	$2\pm1$	$54\pm5$
$K^-p2\pi^+2\pi^-\pi^\pm\pi^0$	$71\pm5$	$13\pm2$	$6\pm1$
	$52\pm4$	$5\pm1$	$3\pm1$
$\pi^-p3\pi^+2\pi^-\bar{K}^0$	$15\pm4$	$63\pm10$	$7\pm3$
	$6\pm2$	$42\pm7$	$6\pm3$
$K^-3\pi^+3\pi^-n$	$9\pm3$	$9\pm3$	$66\pm11$
	$3\pm1$	—	$56\pm10$
$K^-pK^+K^-\pi^\pm\pi^0$	$12\pm2$	$20\pm3$	$13\pm2$
	$7\pm2$	$9\pm2$	$10\pm2$



TABLE II

Probability (in %) that events obtained from passing suitable 4c fit events, truncated to two or more neutral particle types given in the first row, through kinematical fitting, would be assigned incorrectly to the 1c fit reactions indicated in heading, after application of various selection criteria. The selection criteria and the meaning of the upper and lower sets of figures for each simulated reaction are the same as in Table I.

Rough estimates of the cross sections for each multineutral channel are also given

1c fit hypotheses assigned according to selection criteria		$K^-p+\pi^0$ + charged $\pi$ mesons (%)	$\pi^-p+\bar{K}^0$ + charged $\pi$ mesons (%)	$K^-\pi^++n$ + charged $\pi$ mesons (%)
Channels simulated	$\sigma_{\text{est}}(\mu b)$			
$K^-p2\pi^0$	250	$12 \pm 1$ $6 \pm 1$	$14 \pm 1$ $11 \pm 1$	$1 \pm 1$ $1 \pm 1$
$\pi^-p\bar{K}^0\pi^0$	250	$10 \pm 1$ $9 \pm 1$	$5 \pm 1$ $5 \pm 1$	— —
$K^-\pi^+n\pi^0$	300	— —	— —	$14 \pm 1$ $14 \pm 1$
$K^-p\pi^\pm 3\pi^0$	150	$1 \pm 1$ —	$2 \pm 1$ $1 \pm 1$	$3 \pm 1$ $3 \pm 1$
$2\pi^-p\bar{K}^02\pi^0$	250	$4 \pm 1$ $4 \pm 1$	— —	$1 \pm 1$ $1 \pm 1$
$K^-2\pi^+n2\pi^0$	300	— —	— —	$3 \pm 1$ $3 \pm 1$
$K^-p\pi^+\pi^-2\pi^0$	450	$10 \pm 1$ $5 \pm 1$	$14 \pm 1$ $10 \pm 1$	$4 \pm 1$ $3 \pm 1$
$\pi^-p\pi^+\pi^-\bar{K}^0\pi^0$	240	$12 \pm 1$ $10 \pm 1$	$5 \pm 1$ $5 \pm 1$	$2 \pm 1$ $2 \pm 1$
$K^-2\pi^+\pi^-n\pi^0$	300	$1 \pm 1$ $1 \pm 1$	$1 \pm 1$ —	$16 \pm 1$ $15 \pm 1$
$2\pi^+2\pi^-\bar{K}^0n$	60	$2 \pm 1$ $1 \pm 1$	— —	$4 \pm 1$ $3 \pm 1$
$K^-p\pi^+\pi^-\pi^\pm 3\pi^0$	330	— —	— —	$4 \pm 1$ $4 \pm 1$
$\pi^-p2\pi^+\pi^-\bar{K}^02\pi^0$	230	$6 \pm 1$ $4 \pm 1$	— —	$3 \pm 1$ $3 \pm 1$
$3\pi^+3\pi^-\bar{K}^0n\pi^0$	80	$2 \pm 1$ $1 \pm 1$	— —	$5 \pm 1$ $5 \pm 1$
$K^-p2\pi^+2\pi^-2\pi^0$	430	$9 \pm 1$ $6 \pm 1$	$14 \pm 1$ $8 \pm 1$	$10 \pm 1$ $7 \pm 1$
$\pi^-p2\pi^+2\pi^-\bar{K}^0\pi^-0$	130	$19 \pm 2$ $17 \pm 2$	$3 \pm 1$ $2 \pm 1$	$8 \pm 1$ $8 \pm 1$
$K^-3\pi^+2\pi^-n\pi^0$	150	$3 \pm 1$ $2 \pm 2$	$3 \pm 1$ $1 \pm 1$	$11 \pm 2$ $11 \pm 2$
$3\pi^+3\pi^-\bar{K}^0n$	50	$8 \pm 3$ $8 \pm 3$	$2 \pm 1$ $2 \pm 1$	$5 \pm 2$ $5 \pm 2$

corresponding quantities at 32 GeV/c, and taking into account the tendency for probability of the production of several  $\pi^0$ 's to increase as energy increases we calculated that

$$(A + 2\pi^0)/(A + \pi^0) = 1.0, \quad (A + 3\pi^0)/(A + \pi^0) = 0.7, \quad (A + 4\pi^0)/(A + \pi^0) = 0.3,$$

where  $A$  is the final state without  $\pi^0$  mesons.

Estimates of the cross sections for channels with several neutral particles used in this analysis are given in Table II.

It is evident that if the relative probability of misidentification among given competing channels is sufficiently small, the choice of the size of the corresponding cross section is not especially crucial for the calculation of the contamination and loss of 1c fit hypotheses.

Thus insufficiently accurate knowledge of the cross sections for certain final states with several neutral particles, considered in estimating the errors of the determination of the cross sections for channels (1) and (2), did not lead to a significant increase of the errors of the corresponding cross sections.

We note in addition that if in a given reaction neutral particles are present which can be detected, in case they are associated with an event, this event cannot contaminate a 1c fit channel. Therefore the majority of the cross sections for test channels were multiplied by coefficients  $\beta_k$  which took into account unseen decay modes, average potential weight and the effective passing rate for  $V^0$  or  $\gamma$  for the data reduction system which was used in this experiment.

To evaluate the actual cross sections of the 1c fit reactions investigated, the following system of equations was solved

$$\sigma_{iu}\beta_i = \alpha_{ii}\beta_i\sigma_{ir} + \sum_{j=i+1}^N \alpha_{ij}\beta_j\sigma_{jr},$$

where  $\sum_{j \neq i=1}^N \alpha_{ij}\beta_j\sigma_{jr}$  — amount of contamination in the  $i$ -th 1c fit channel (separation error of the second type;  $E2$ ),  $(1 - \alpha_{ii})\beta_i\sigma_{ir}$  — loss (separation error of the first type;  $E1$ ),  $\sigma_{iu}$  — uncorrected value of the cross section of the  $i$ -th 1c fit channel with the given method of separation of hypotheses,  $\sigma_{ir}$  — real value of the cross section of the  $i$ -th 1c fit channel,  $\alpha_{ij}$  — probability of misidentification from  $j$ -th to  $i$ -th reaction channel. To estimate the misidentification probabilities data from Tables I and II were used with some additional simplifying assumptions.

Results for the cross sections of reactions (1)–(4) are given in Table III. For comparison purposes the cross sections for the same reactions derived from 7c fit events (for example, channels with a seen  $\bar{K}^0$  meson) or 5c fit events (events to which one  $\gamma$ -quantum from a  $\pi^0$  meson decay is associated, and a second  $\gamma$ -quantum is reconstructed using the additional constraint equation  $M_{\gamma\gamma} = m_{\pi^0}$ ) are also given in this table. From Table III it is seen that the results of the calculation of the cross sections by the method described above with corrections for loss ( $E1$ ) and contamination ( $E2$ ) are in reasonably good agreement with the cross sections obtained for 7c fit and 5c fit events. An exception is the channel  $K^-p \rightarrow K^0p\pi^-\pi^0$ . The cross section for this channel has been corrected for the loss of events with short recoil protons by extrapolating the momentum transfer distribution. We note that cross sections for 5c fit events were calculated according to the first

TABLE III

Summary of the cross sections for reactions (1)–(4) obtained by the method described in the text, and comparison to 5c fit and 7c fit channels when possible. The corrected value for the 1c fit cross sections,  $\sigma_{\text{cor}}$ , are obtained from the uncorrected values  $\sigma_{\text{uncor}}$  by subtracting the contaminations ( $E2$ ) and adding the estimated losses ( $E1$ )

Charged multiplicity $N_{\text{ch}}$	Channel	1c fit				$\sigma_{\text{cor}}$ ( $\mu\text{b}$ )	5 and 7c fit	
		Number of ev-s	$\sigma_{\text{uncor}}$ ( $\mu\text{b}$ )	Contamination $E2$ ( $\mu\text{b}$ )	Loss $E1$ ( $\mu\text{b}$ )		Number of ev-s	$\sigma(\mu\text{b})$
2	$\text{K}^- \text{p} \pi^0$	557	$216 \pm 9$	$92 \pm 9$	$44 \pm 8$	$169 \pm 19$	48	$122 \pm 17$
	$\bar{\text{K}}^0 \text{p} \pi^+ \pi^0$	136	$258 \pm 19$	$38 \pm 4$	$61 \pm 9$	$281 \pm 27$	41	$593 \pm 92$
	$\bar{\text{K}}^0 \text{p} \pi^-$	117	$52 \pm 4$	$31 \pm 5$	$19 \pm 6$	$41 \pm 13$	36	$51 \pm 8$
	$\text{K}^- \pi^+ \text{n}$	726	$245 \pm 9$	$103 \pm 8$	$62 \pm 12$	$205 \pm 23$	—	—
4	$\text{K}^- \text{p} \pi^+ \pi^- \pi^0$	1117	$495 \pm 14$	$132 \pm 10$	$115 \pm 11$	$478 \pm 26$	140	$439 \pm 37$
	$\bar{\text{K}}^0 \text{p} \pi^+ 2\pi^- \pi^0$	129	$217 \pm 19$	$36 \pm 4$	$54 \pm 10$	$236 \pm 27$	15	$212 \pm 54$
	$\bar{\text{K}}^0 \text{p} \pi^+ 2\pi^-$	192	$102 \pm 7$	$42 \pm 6$	$70 \pm 12$	$130 \pm 22$	66	$102 \pm 11$
	$\text{K}^- \text{n} 2\pi^+ \pi^-$	719	$277 \pm 10$	$137 \pm 12$	$68 \pm 11$	$207 \pm 26$	—	—
6	$\text{K}^- \text{p} 2\pi^+ 2\pi^- \pi^0$	972	$455 \pm 14$	$98 \pm 10$	$104 \pm 14$	$461 \pm 28$	134	$433 \pm 37$
	$\bar{\text{K}}^0 \text{p} 2\pi^+ 3\pi^- \pi^0$	71	$122 \pm 14$	$27 \pm 4$	$27 \pm 7$	$122 \pm 21$	14	$176 \pm 47$
	$\bar{\text{K}}^0 \text{p} 2\pi^+ 3\pi^-$	125	$71 \pm 6$	$27 \pm 4$	$65 \pm 14$	$109 \pm 22$	24	$50 \pm 7$
	$\text{K}^- \text{n} 3\pi^+ 2\pi^-$	350	$142 \pm 7$	$106 \pm 8$	$19 \pm 7$	$56 \pm 17$	—	—

hypothesis with the restriction that  $-1.5 \text{ GeV}^2 < M_{\text{mis}}^2(\gamma) < 1.5 \text{ GeV}^2$  and  $P(\chi^2) > 0.001$ . For further analysis we will use the values for cross sections obtained for 1c fit events. From Table III it is seen that for the channels  $\text{K}^-p \rightarrow \text{K}^-p + m(\pi^+\pi^-)$  with  $m \geq 1$  the method described above provides a clean enough separation (with contamination  $< 25\%$ ), however, the separation of analogous channels with a  $\bar{\text{K}}^0$  meson is very difficult due to their small cross sections and large overlap between (1) and (3).

In Fig. 4 and 5 the  $P_{\text{lab}}$  dependence of the cross sections of reactions (1) and (3) is shown. The solid lines in the figure connect the experimental points belonging to the

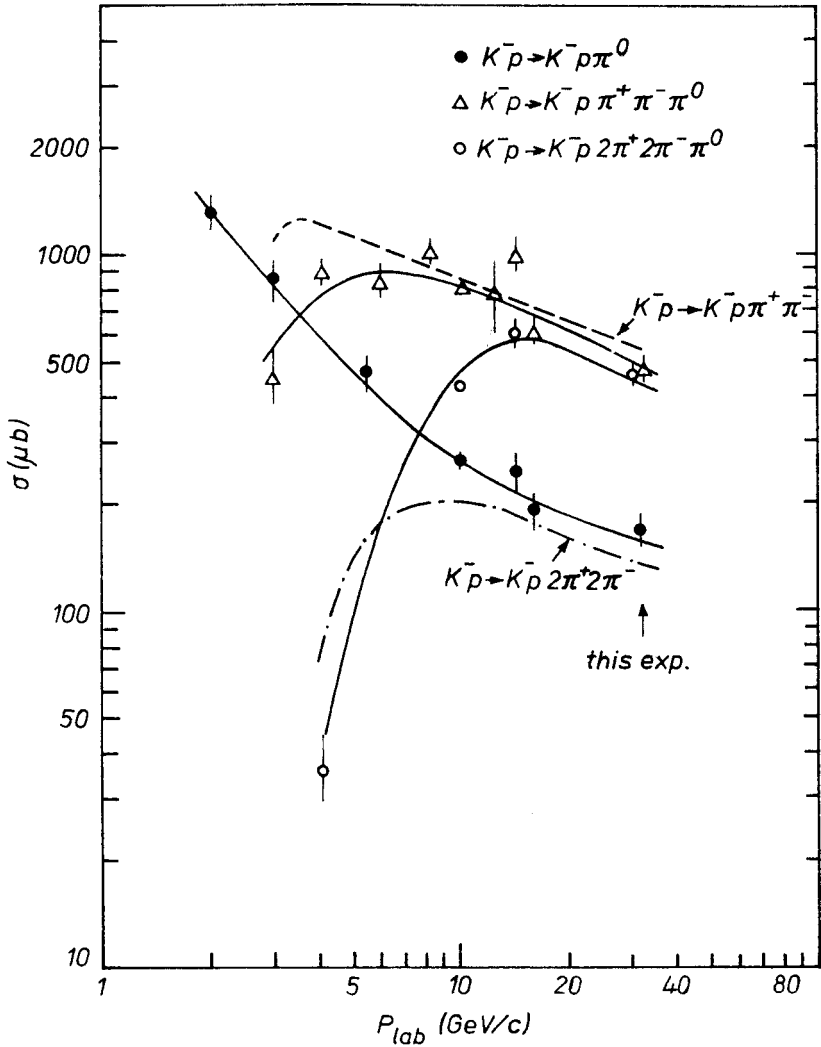


Fig. 4. Energy dependence of reactions (1) for  $m = 0, 1, 2$ . The solid lines show the general trend of the  $P_{\text{lab}}$  dependence of the given 1c fit channels. The dotted and dashed lines show the behaviour of 4c fit channels without a  $\pi^0$  meson

same channel. The dotted and dashed curves show the behavior of nearby 4c fit channels. These curves are taken from Ref. [8] and values for the cross sections at lower energies.

As seen in Fig. 4 for  $P_{\text{lab}} > 10 \text{ GeV}/c$  the cross sections for the channels  $K^-p \rightarrow K^-p\pi^+\pi^-$  and  $K^-p \rightarrow K^-p\pi^+\pi^-\pi^0$  nearly coincide and have similar energy dependence. For analogous states with  $2(\pi^+\pi^-)$  pairs the cross section for states with an additional  $\pi^0$  meson at  $32 \text{ GeV}/c$  is three times larger than the cross section for the corresponding 4c fit channel. Such a difference in the ratios of the 4c fit and 1c fit channels between 4 and 6 prong events can be explained by the large contribution of single diffraction to the reaction  $K^-p \rightarrow K^-p\pi^+\pi^-$ .

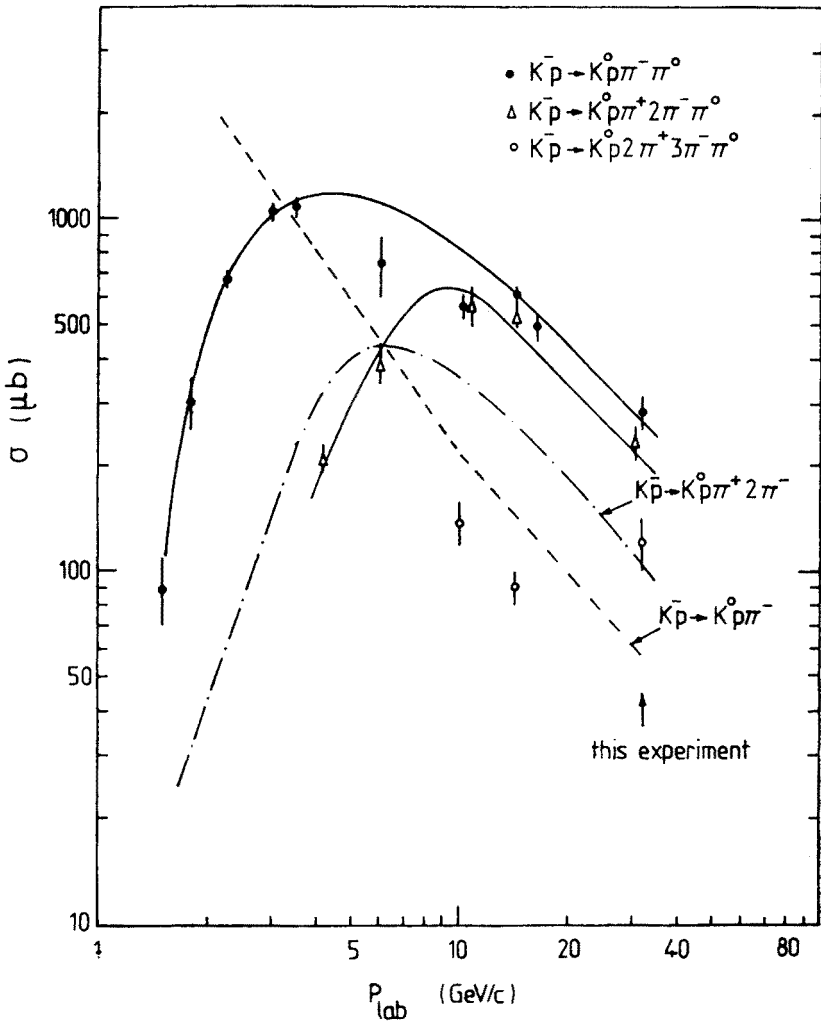


Fig. 5. Energy dependence of reactions (2) with  $m = 0, 1, 2$ . The solid, dotted and dashed lines have the same meanings as in Fig. 4 for this reaction type

In reactions with neutral kaons the cross section for reaction (2) is considerably larger than the cross section for the corresponding reaction without  $\pi^0$  mesons (by a factor of 2–4).

Thus at energies in the 30 GeV region the separation of multiprong 1c fit states presents new possibilities for the investigation of the structure of exclusive states as the cross sections for exclusive 4c fit channels at this energy are considerably smaller than the corresponding 1c fit channels.

#### 4. Summary and conclusions

As this work has shown, the accuracy of measurement of the kinematic parameters of particles in the 32 GeV/c  $K^-p$  experiment permits a reliable enough separation of exclusive channels with one unseen  $\pi^0$  for charged particle multiplicity 4 and larger. The separation of channels with an unseen  $\bar{K}^0$  is complicated by the large contamination from kinematically inseparable reactions with 1 and  $2\pi^0$  mesons and the relatively small cross sections of such channels.

The results obtained permit the addition of about 5000 1c fit events to the study of 4c fit events.

The energy dependence of the cross sections for channels with one  $\pi^0$  meson in 4 and 6 prong events is analogous to the behaviour of the cross sections of the corresponding channels without  $\pi^0$  mesons at  $P_{\text{lab}} > 10$  GeV/c.

#### REFERENCES

- [1] D. Hansen et al., CERN preprint (D. ph. II) Phys. 74–44.
- [2] D. R. O. Morrison et al., CERN preprint (EP) Phys. 77–3.
- [3] P. F. Ermolov et al., IHEP preprint 72–68, Serpukhov 1969; P. E. Ermolov et al., IHEP preprint 72–69, Serpukhov 1969.
- [4] M. Y. Bogolyubskii et al., IHEP preprint 76–108, Serpukhov 1976; English version: *A Simple Method for Calculation of Systematic Distortions in Bubble Chambers*, translated by J. MacNaughton, Institut für Hochenergiephysik der Österreichischen Akademie der Wissenschaften, Vienna.
- [5] C. Cochet et al., *Nucl. Phys.* **B124**, 61 (1977).
- [6] G. Pietrzijk, *Etude de la dissociation diffractive du Proton dans les interactions  $K^-p$  à 14,3 GeV/c*. Thèse présentée à l'université de Paris VI (1974).
- [7] J. R. Elliot et al., *Nucl. Phys.* **B133**, 1 (1978).
- [8] A. Givernaud et al., *Nucl. Phys.* **B160**, 445 (1979).